jove

Improving the Combustion Performance of a Hybrid Rocket Engine using a Novel Fuel Grain with a Nested Helical Structure

Zezhong Wang[1,2], **Xin Lin**[1], **Fei Li**[1], **Zelin Zhang**[1], **Xilong Yu**[1,2]

[1] Institute of Mechanics, Chinese Academy of Sciences [2] School of Engineering Science, University of Chinese Academy of Sciences

Corresponding Author

Xin Lin
linxin_bit@163.com

Citation

Wang, Z., Lin, X., Li, F., Zhang, Z., Yu, X. Improving the Combustion Performance of a Hybrid Rocket Engine using a Novel Fuel Grain with a Nested Helical Structure. *J. Vis. Exp.* (167), e61555, doi:10.3791/61555 (2021).

Date Published

January 18, 2021

DOI

10.3791/61555

URL

jove.com/video/61555

Abstract

A technique to improve the combustion performance of a hybrid rocket engine using a novel fuel grain structure is presented. This technique utilizes the different regression rates of acrylonitrile butadiene styrene and paraffin-based fuels, which increase the exchanges of both matter and energy by swirl flow and recirculation zones formed at the grooves between the adjacent vanes. The centrifugal casting technique is used to cast the paraffin-based fuel into an acrylonitrile butadiene styrene substrate made by three-dimensional printing. Using oxygen as the oxidizer, a series of tests were conducted to investigate the combustion performance of the novel fuel grain. In comparison to paraffin-based fuel grains, the fuel grain with a nested helical structure, which can be maintained throughout the combustion process, showed significant improvement in the regression rate and great potential in improvement of combustion efficiency.

Introduction

A technique to improve the combustion performance of a hybrid rocket engine is urgently required. To date, practical applications of hybrid rocket engines are still far less than those of solid and liquid rocket engines[1,2]. The low regression rate of traditional fuels limits the improvement of thrust performance for the hybrid rocket engine[3,4]. In addition, its combustion efficiency is slightly lower than that of other chemical energy rockets due to internal diffusion combustion[5], as shown in **Figure 1**. Although various techniques have been studied and developed, such as the use of multi-ports[6], enhancing additives[7,8,9], liquefying fuel[10,11,12], swirl injection[13], protrusions[14], and bluff body[15], these approaches are associated with problems in volume utilization, combustion efficiency, mechanical performance, and redundancy quality. Thus far, structural improvement of the fuel grain, which does not have these shortcomings, has attracted more attention as an effective means of

improving combustion performance[16,17]. The advent of three-dimensional (3D) printing has brough an effective way to increase the performance of hybrid rocket engines through the ability to rapid and inexpensively produce either complex conventional grain designs or nonconventional fuel grains[18,19,20,21,22,23,24,25,26,27,28,29,30]. However, during the combustion process, these improvements in combustion performance diminishes with the characteristic structure burning, resulting in a decrease in combustion performance[23]. We have demonstrated that a novel design is useful in improving performance of hybrid rocket engines[31]. The detail for this technique and representative results is presented in this paper.

The fuel grain consists of a helical substrate made by acrylonitrile-butadiene-styrene (ABS) and a nested paraffin-based fuel. Based on centrifugal and 3D printing, the advantages of the two fuels with different regression rates were combined. The special helical structure of the fuel grain after combustion is shown in **Figure 2.** When gas passes through the fuel grain, numerous recirculation zones are simultaneously created at grooves between blades, which is shown in **Figure 3**. This characteristic structure on the inner surface increases the turbulence kinetic energy and swirl number in the combustion chamber, which increase the exchanges of both matter and energy in the combustion chamber. Ultimately, the regression rate of the novel fuel grain is effectively improved. The effect of improving the regression rate has been well proven: in particular, the regression rate of the novel fuel grain was demonstrated to be 20% higher than that of the paraffin-based fuel at the mass flux of 4 g/s·cm^2[2,32].

One advantage of the fuel grain with a nested helical structure is that it is simple to manufacture. The molding process mainly requires a melt mixer, a centrifuge, and a 3D printer. The ABS substrate formed by 3D printing greatly reduces the manufacturing cost. Another significant and unique advantage is that the enhancement effect does not disappear during the combustion process.

This paper presents the experimental system and procedure for improving the combustion performance of a hybrid rocket engine using the novel fuel grain structure. Additionally, this paper presents three representative comparisons of combustion performance parameters to prove the feasibility of the technique, including oscillation frequency of combustion chamber pressure, regression rate, and combustion efficiency characterized by characteristic velocity.

Protocol

1. Experimental setup and procedures

1. Preparation of fuel grain

   NOTE: The fuel grain with novel structure consisted of two parts, which are shown in **Figure 4**. As the main part of the novel grain, the paraffin-based fuel accounts for more than 80% of the total mass. The ABS substrate is used as an additional fuel. The preparation of this fuel grain was realized by combining 3D printing and centrifugal casting.

   1. Substrate preparation

      1. Open 3D software for ABS substrate drawing.

         NOTE: The ABS substrate, which intended to provide the helical framework and support for the paraffin-based fuel, is comprised of twelve integrated blades that rotate 360° clockwise in the axial direction and the wall.

2. Save the 3D structure of the ABS substrate as a **STL** file.
3. Open the 3D slicing software and import the structure of ABS substrate.
4. Click **Start Slicing**, and select **Speed** print mode from **Main Template**.
   NOTE: For the **Primary Extruder** choose **ABS 1.75 mm**.
5. Double-click **Speed**, change the infill density to 100% and select **Raft with Skirt** for the **Platform Addition**.
   NOTE: In order to improve the print quality and prevent warping, it is necessary to use a structure of print base (**Raft with Skirt**) to increase the contact area between the print body and the bottom plate.
6. Click **Save and Close**, and then click **Slice**.
7. Turn on the 3D printer and import the ABS substrate slice file.
8. Set the temperature of the heated bed and nozzle to 100 and 240 °C, respectively.
9. Click **Start** to print after stabilization.

2. Paraffin-based fuel preparation
   1. Prepare raw materials of paraffin, polyethylene (PE) wax, stearic acid, ethylene-vinyl acetate (EVA), and carbon powder. Configure the paraffin-based fuel according to the ratio of these components as 0.58:0.2:0.1:0.1:0.02.
      NOTE: The specific information of each raw material is shown in the material table. The distribution ratio of paraffin-based fuel is not fixed and can be adjusted appropriately according to the purpose of the experiment. The purpose of adding carbon powder is to block radiant heat transfer and prevent the fuel grain from softening and collapsing during combustion.
   2. Place the configured raw materials into the melt mixer, and fully melt and stir until completely mixed.
      NOTE: The paraffin-based fuel is heated to 120 °C to ensure complete melting while preventing deformation of the ABS blades.

3. Fuel grain manufacturing
   NOTE: To better demonstrate the effect of improving the combustion performance, paraffin-based fuel grains with the same composition were set as the control.
   1. Place the ABS substrate into the centrifuge, and secure it with an end cap.
   2. Plug in the power and turn on the water-cooling pump switch.
   3. Turn on the centrifuge relay and increase the speed to 1400 rpm.
   4. Open the valve on the melt mixer and start casting.
      NOTE: The molten paraffin-based fuel flows into the initial section of mold through the pipe and the end cover with a central opening. Under the effect of gravity, the liquid fuel spreads along the axial direction of the mold. Combined with effective cooling, a multiple-casting method, which is to divide the original one-time filling process into multiple times, is required to reduce the thermal stress.

5. Remove the fuel grain and trim the shape.

4. Fuel grain measurement and recording

1. Measure and record the weight, length, and inner diameter of the fuel grain.

2. Photograph the complete fuel grain.

2. Preparation of hybrid rocket engine system

NOTE: As shown in **Figure 5**, the hybrid rocket engine system consisted of four parts: the supply system, the ignition system, the engine, and the measurement and control system. The engine part included five parts: the torch igniter, the head, the combustion chamber, the post-combustion chamber, and the nozzle. The total length of the hybrid rocket engine is about 300 mm, and the inner diameter of the combustion chamber is 70 mm.

1. Hybrid rocket engine assembly

NOTE: The exhaustive details of the laboratory-scale hybrid rocket and the composition of the experimental system can be found in the previous paper[32].

1. Fix the combustion chamber section of hybrid rocket engine on the slide rail.

2. Load the fuel grain and install the post-combustion chamber section.

3. Install the head and nozzle.

4. Install the torch igniter on the head of the hybrid rocket engine.

5. Install the spark plug and connect the power supply.

2. Connect the nitrogen, oxidizer, ignition methane, and ignition oxygen gas supply lines between the test bench and the gas cylinder.

3. Connect the industrial computer, the multi-function data acquisition card, the mass flow controller, and the control box of the test bench.

4. Power on the test bench, the mass flow controller, and the igniter.

3. Check the test system and set the experimental conditions.

1. Open the **FlowDDE** software and click **Communications settings** from the **Communication.**

2. Click the corresponding connection interface and click **OK.**

3. Click **Open communication** to establish communication with the flow controller and open the measurement and control program (MCP).

4. Set the I/O channel of the multi-function data acquisition card and click **Run** to establish communication with the entire system.

5. Check MCP running status and set to manual control mode.

NOTE: The MCP includes two modes: manual control is used for debugging and automatic control is used during experiments. The MCP written by LabVIEW is shown in **Figure 6**.

6. Check the working condition of the spark plug and perform a valve test.

7. Test data recording function.

8. Open the setting interface and set test time, including valve opening and closing time, ignition time, and data recording duration.

NOTE: It takes some time for the mass flow controller to regulate the oxidizer flow to the set

value, so the ignition time was set to 2 s after the supply of oxidizer.

9. Set safety requirements and clear personnel from the experimental area.

10. Open the cylinder valve and adjust the output pressure of the regulating valve according to the different mass flow rate conditions.

NOTE: With the supply pressure of 6MPa, the range of mass flow rate of the oxidizer is between 7 g/s and 29 g/s.

11. Open the setting interface and set the oxidizer mass flow rate.

4. Hybrid rocket engine ignition

1. Turn on the camera.

2. Set the MCP to automatic control mode and wait for trigger.

3. Click **Start** on the MCP to start the experiment.

4. After about one minute, click **Stop** on the MCP and turn off the camera.

5. Close the gas cylinder and open the valve in the pipeline to relieve the pressure.

6. Power off the test bench and remove the fuel grain.

7. Repeat Step 1.1.4.

2. Analysis of combustion performance

1. Analysis of pressure oscillation

NOTE: The saved combustion chamber pressure data is represented as $P_C(t)$.

1. Open $P_C(t)$ with the data processing software.

2. Choose the time period during the combustion process of the hybrid rocket engine.

3. Select **Analysis > Signal Processing > FFT** to analyze the pressure oscillation.

4. Use the default settings and click **OK.**

2. Analysis of regression rate

1. Calculate the regression rate of the fuel grain according to the following function:

$$\dot{r} = \frac{\Delta D}{2t} = \frac{\sqrt{{d_0}^2 + \frac{4\Delta m_f}{\pi \rho L}} - d_0}{2t}, \quad (1)$$

where ΔD represent the change of average inner diameters of the solid fuel grain after the firing test; Δm_f represent the change of quality of the fuel grain; L is the length of the fuel grain; ρ is the average density of the solid fuel; t is the working time.

NOTE: The average density ρ of the novel grain was expressed as:

$$\rho = \rho_p \omega_p + \rho_{ABS} \omega_{ABS}, \quad (2)$$

where ρ_p and ρ_{ABS} represent the density of the nested paraffin-based fuel and ABS material, respectively; ω_p and ω_{ABS} represent the mass fraction of the nested paraffin-based fuel and ABS material, respectively.

2. Fit the regression rate as a function of oxidizer flux.

NOTE: The fitting function was selected as Allometric1 $(y = ax^b)$, and the iterative algorithm was selected as Levenberg–Marquardt optimization algorithm.

3. Analysis of combustion efficiency

1. Calculate average combustion chamber pressure P_C by the following function:

$$P_c = \frac{\sum_{t=t_1}^{t_n} P_c(t)}{n}, \quad (3)$$

where $P_C(t)$ represents the combustion chamber pressure at different times; t_1 and t_n represent

the initial and final times at which the combustion chamber pressure was greater than 50% of the average pressure, respectively; n represents the number of pressure data points between and t_1 and t_n.

2. Calculate the combustion characteristic velocity C^* according to the following function:

$$C^* = \frac{P_c A_t}{\dot{m}}, \quad (4)$$

where P_c is the average combustion chamber pressure; A_t is the throat area; $\dot{m}$ is the total mass flow rate.

3. Calculate the theoretical characteristic velocity of paraffin fuel C^*_P by NASA CEA code[33].

Representative Results

Figure 7 shows the changes in combustion chamber pressure and oxidizer mass flow rate. To provide the necessary time for flow regulation, the oxidizer enters the combustion chamber in advance. When the engine builds pressure in the combustion chamber, the oxygen mass flow rate drops rapidly and then maintains a relatively steady change. During the combustion process, the pressure in the combustion chamber remains relatively stable.

Images showing a comparison of combustion chamber pressure oscillation frequency are presented in **Figure 8**. The pressure fluctuation spectrum of the novel fuel grain contained three distinct peaks, which were associated with the hybrid low frequency, Helmholtz mode and the acoustic half-wave in the combustion chamber, respectively[34]. The position of the pressure peaks corresponding to the novel fuel grain were basically the same as that of the paraffin-based fuels, which indicates that novel structure is not likely to introduce additional combustion oscillations. Moreover, it can be clearly seen from the smoothed curve that the amplitude of dominant low-frequency pressure oscillation was slightly amplified by the novel structure. Therefore, before the actual application of the novel fuel grain, further structural optimization is needed to reduce the amplitude of pressure oscillations.

Figure 9 shows a comparison of regression rate as a function of oxidizer flux between novel fuel grains and paraffin-based fuel grains. Compared with traditional HTPB fuels, the regression rate of paraffin-based fuels was approximately doubled. Nevertheless, at the same oxidizer mass flow rate, the regression rate of the novel fuel grain was demonstrated to be higher than that of the paraffin-based fuel. And the gap between the regression rates of two fuels also gradually widened as the oxidizer flux increased.

An image comparing combustion efficiency based on the characteristic velocity is presented in **Figure 10**. The novel fuel grain exhibited a higher (characteristic velocity) than paraffin-based grains at various oxidizer/fuel ratios. Correspondingly, facilitated by the nested helical structure, the average combustion efficiency of the novel fuel grain has been increased by about 2% (±0.7%). Due to the low calorific value of commercial ABS materials and the different equivalence ratios, the improvement of the combustion efficiency brought by the novel structure was not obvious.

The results of firing tests demonstrated that the performance of the regression rate for the fuel grain with a nested helical structure could be effectively improved[32]. Moreover, the novel structure also shows a great potential in improvement of combustion efficiency. Both numerous recirculation zones at the grooves between adjacent vanes and the helical structure increases the turbulence and swirl number in the combustion

chamber. The exchange of matter and energy between the fuel grain and the combustion zone is increased, thereby improving the combustion performance.

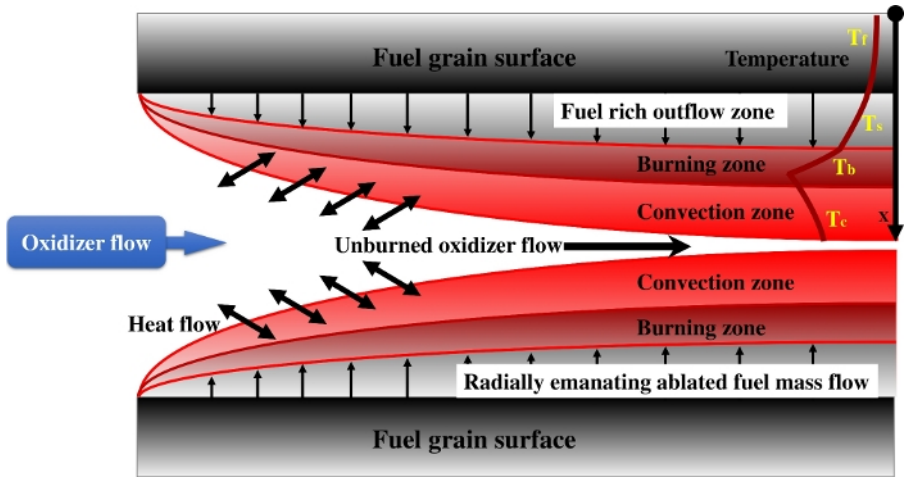

Figure 1: Combustion process involved in hybrid rocket.

The mixing and combustion processes of the hybrid rocket is different from either liquids or solids. In hybrids, mixing and combustion occur in the area of diffusion combustion that has the same length as the combustion chamber. The nature of the diffusion combustion model leads to a reduction in the degree of mixing and combustion efficiency, which ranges from 50% to 99% in practical applications[27,35]. Please click here to view a larger version of this figure.

Figure 2: Characteristic structure of novel fuel grain.

Owing to the different regression rates between two fuels, this nested helical structure is formed and maintained during the combustion process. Please click here to view a larger version of this figure.

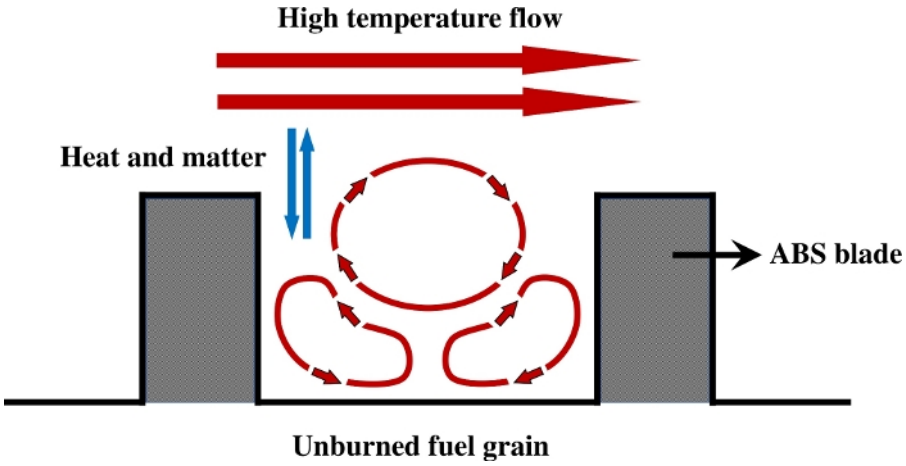

Figure 3: Recirculation zone formed.

When gas passes through the grooves between adjacent vanes, a recirculation zone is formed. Disturbance is intensified, and the exchanges of matter and energy in the combustion chamber have been enhanced. Please click here to view a larger version of this figure.

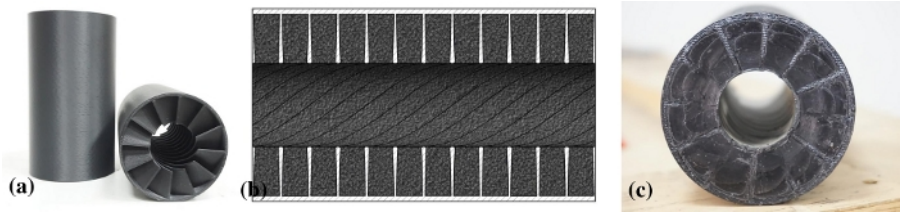

Figure 4: Structural images of novel fuel grain.

(**a**) 3D printing of ABS substrate with an outer diameter of 70 mm, an inner diameter of 30 mm, and a length of 125 mm. (**b**) Nested helical structure of the novel fuel grain, in which paraffin-based fuel and ABS blades maintain the same initial inner diameter. (**c**) Image of the shaped fuel. Please click here to view a larger version of this figure.

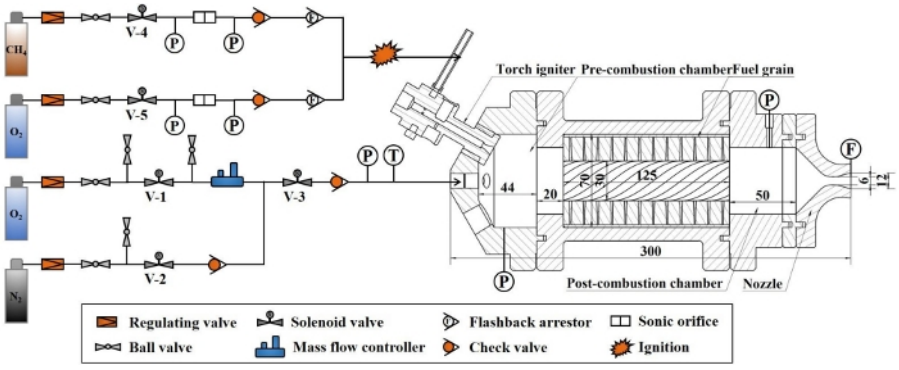

Figure 5: Experimental setup.

Schematic of the laboratory-scale hybrid rocket engine. Please click here to view a larger version of this figure.

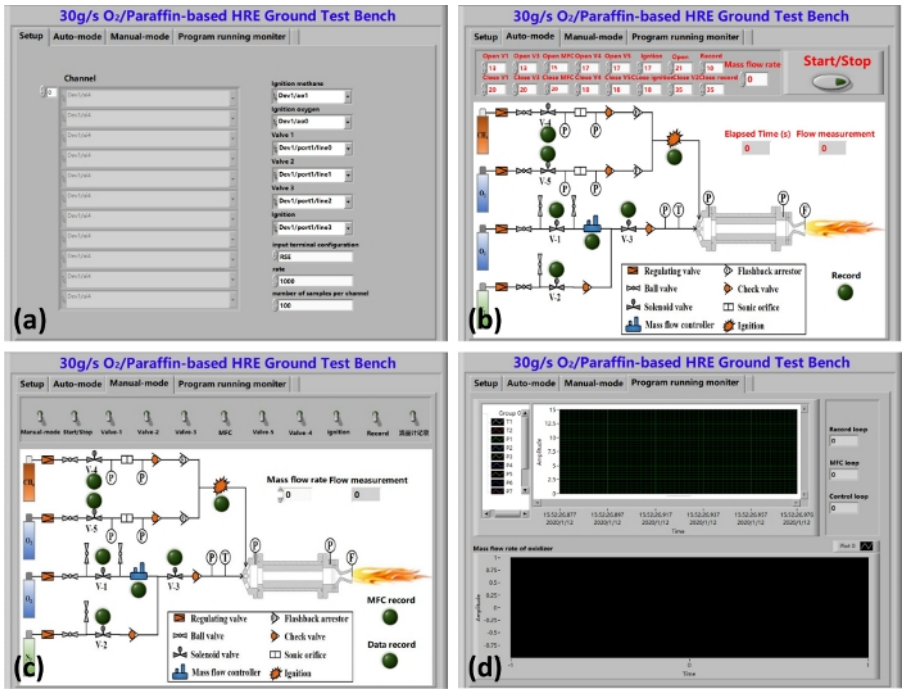

Figure 6: LabVIEW measurement and control program interface.

(**a**) Setup interface (**b**) auto-mode interface (**c**) manual-mode interface (**d**) program running monitoring interface. Please click here to view a larger version of this figure.

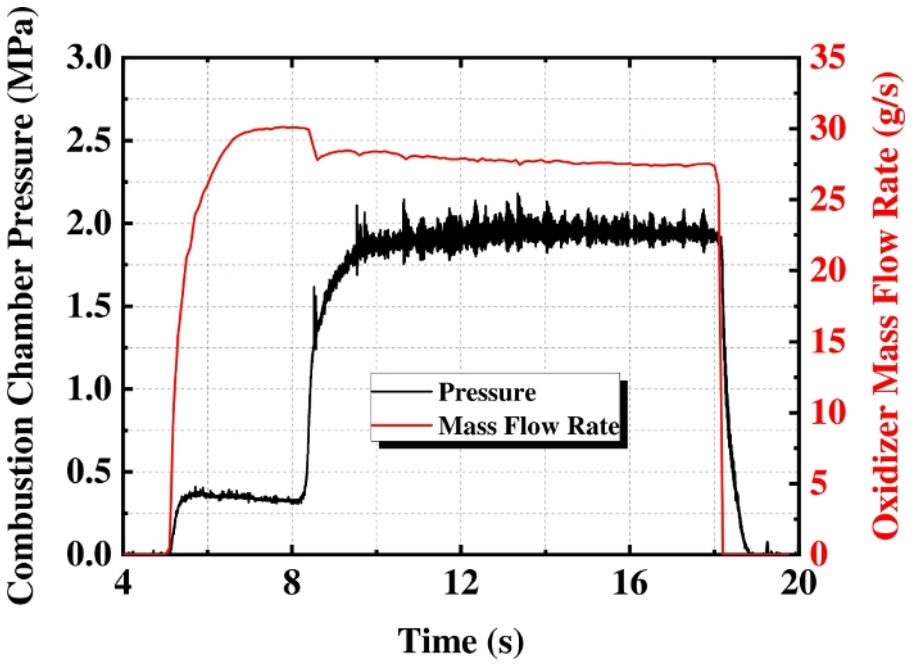

Figure 7: Change of combustion chamber pressure and oxidizer mass flow rate.

During the combustion process, the mass flow rate of oxidizer and combustion chamber pressure remain relatively stable.

Please click here to view a larger version of this figure.

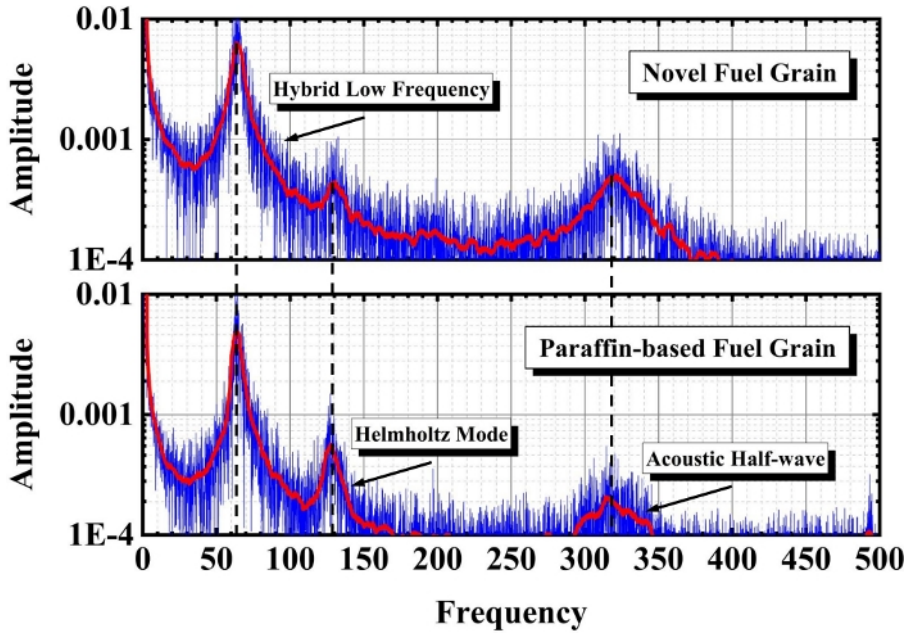

Figure 8: Comparison of combustion chamber pressure oscillation frequency.

Low frequency oscillation is the dominant combustion oscillation mode of hybrid rockets. Compared with paraffin-based fuel grains, the amplitude of dominant oscillation for the fuel grain with nested helical structure has slightly increased. Please click here to view a larger version of this figure.

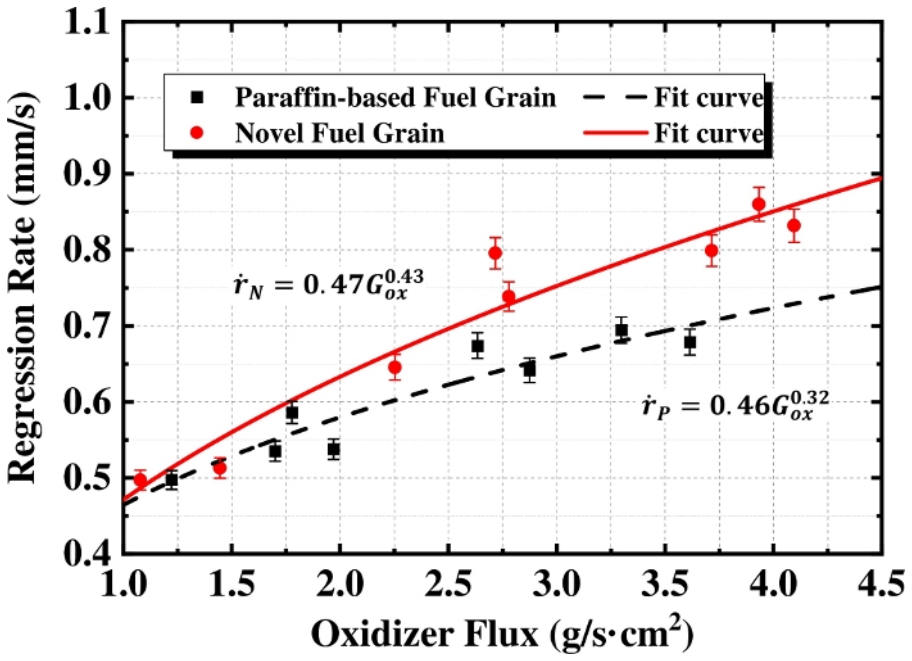

Figure 9: Comparison of regression rate with oxidizer flux.

As the flux of the oxidizer increases, the effect of the novel structure on increasing the regression rate becomes more significant. Please click here to view a larger version of this figure.

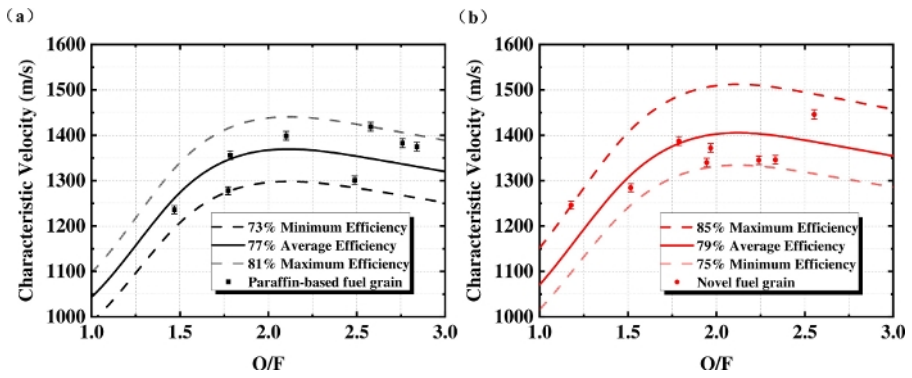

Figure 10: Comparison of combustion efficiency based on characteristic velocity.

(**a**) The average combustion efficiency of paraffin-based fuel grain is 77%. (**b**) The average burning efficiency of new grains is 79%. Because the combustion calorific value of the ABS material used is extremely low, the combustion efficiency is slightly improved. Please click here to view a larger version of this figure.

Discussion

The technique presented in this paper is a novel approach using a fuel grain with a nested helical structure. There are no difficulties in setting up the necessary equipment and facilities. The helical structure can be easily produced by 3D printing, and nesting of paraffin-based fuels can be easily carried out by centrifugal casting. Fused deposition molding (FDM) 3D printers are not expensive and the cost of centrifuges is low.

When the inner surface of the shaped fuel grain was found to have cracks that cannot be ignored, the heating temperature in the melt mixer was increased to 200 °C. Then, the low-viscosity characteristics of the paraffin-based fuel were used to perform a repair pouring to fill the voids of the fuel grain. After the grain was completely cooled down, the inner hole was polished until the diameter was consistent with the original design one.

There are several critical steps in the protocol. In Step 1.1.1.5, because the contact area between the ABS substrate and print table is small, the bottom of the substrate is easily deformed and can slip during the printing process, which ultimately results in printing failure. This problem can be greatly alleviated by increasing the contact area of the bottom surface. It was found that using the **Raft with Skirt** parameter works best. The infill density must be set to 100% to reduce the printing voids in the ABS substrate and increase the printing density. In addition, in Step 1.1.1.8, setting the heated bed temperature to 100 °C can effectively prevent the ABS substrate from being warped.

In Step 1.1.2.2, based on the thermal deformation temperature of ABS and the minimum melting temperature of the paraffin-based fuel, heating the configured paraffin-based fuel to a temperature of 120 °C was proven feasible. It is necessary to prevent the ABS substrate from deforming when the temperature is too high. At the same time, it is necessary to avoid incomplete melting and mixing of the paraffin-based fuel when the temperature is too low.

In Step 1.1.3, in order to shorten the molding time, and to avoid the problem that the fuel grain is easily cracked due to the excessive thermal stress generated during the cooling process of the one-shot molding process, increasing the number of pourings and effective cooling are necessary for rapid and high-quality molding of the fuel grain. According to the actual molding quality and manufacturing experience, four or more pouring times are required for the size of fuel grain in this work.

There are two limitations to this technique. One is that the materials are incompatible. Due to the thermal stress and casting errors, the novel fuel grain is likely to have cracks, defects or debonding during the casting process. However, by comparing the results of the firing tests between the cracked fuel grain and the normal fuel grain, it was found that the characteristic structure of the two types of fuel grains, which is shown in **Figure 2**, remained basically the same after combustion. No obvious phenomenon of erosive burning was observed on the inner surface of the fuel grain. Because the low viscosity characteristics of the paraffin-based fuel make it spontaneously fill the cracks during the combustion process, this novel fuel grain is not sensitive to cracks.

Second, due to characteristics of centrifuge, paraffin-based fuels are not easily cooled in time during the formation of the fuel grain, resulting in delamination. To avoid such a large impact on the radial uniformity of the fuel grain, increasing the number of pourings can overcome this difficulty.

Based on the structural optimization, a novel fuel grain with a nested helical structure is proposed. Due to the different regression rates between the two materials, this characteristic structure can exist throughout the entire combustion process and provide performance enhancements. Compared with paraffin-based fuel grain, this novel structure shows effective improvement, including the overall regression rate and combustion efficiency.

The presented technique can be used to improve the combustion performance of traditional fuels such as HTPB (hydroxyl-terminated polybutadiene), paraffin-based fuel, and carboxyl-terminated polybutadiene. We believe that this technique can effectively solve the key problem of low regression rate that currently restrict the development of the hybrid rocket engine. In addition, this technique shows great potential for improving combustion efficiency. Further optimization of parameters such as the blade structure, the number of blades, and the blade thickness is needed to maximize the combustion performance.

Disclosures

The authors have nothing to disclose.

Acknowledgments

This work was supported by the National Natural Science Foundation of China (Grant Nos. 11802315, 11872368 and 11927803) and Equipment Pre-Research Foundation of National Defense Key Laboratory (Grant No. 6142701190402).

References

1. Boiron, A. J., Cantwell, B. in *49th AIAA/ASME/SAE/ASEE Joint Propulsion Conference.* (2013).
2. Mazzetti, A., Merotto, L., Pinarello, G. Paraffin-based hybrid rocket engines applications: A review and a market perspective. *Acta Astronautica.* **126**, 286-297 (2016).
3. Karabeyoglu, A., Zilliac, G., Cantwell, B. J., DeZilwa, S., Castellucci, P. Scale-Up Tests of High Regression Rate Paraffin-Based Hybrid Rocket Fuels. *Journal of Propulsion and Power.* **20** (6), 1037-1045 (2004).
4. Jens, E. T., Narsai, P., Cantwell, B., Hubbard, G. S. in *50th AIAA/ASME/SAE/ASEE Joint Propulsion Conference.* (2014).
5. Kuo, K. K., Chiaverini, M. J. *Fundamentals of Hybrid Rocket Combustion and Propulsion.* (2007).
6. Boardman, T. et al. in *33rd Joint Propulsion Conference and Exhibit.* (1997).
7. Connell, T. L. et al. Enhancement of Solid Fuel Combustion in a Hybrid Rocket Motor Using Amorphous Ti–Al–B Nanopowder Additives. *Journal of Propulsion and Power.* **35** (3), 662-665 (2019).
8. Veale, K., Adali, S., Pitot, J., Brooks, M. A review of the performance and structural considerations of paraffin wax hybrid rocket fuels with additives. *Acta Astronautica.* **141** 196-208 (2017).
9. Karakas, H., Kara, O., Ozkol, I., Karabeyoglu, A. M. in *AIAA Propulsion and Energy 2019 Forum.* (2019).
10. Di Martino, G. D., Mungiguerra, S., Carmicino, C., Savino, R. Computational fluid-dynamic modeling of the internal ballistics of paraffin-fueled hybrid rocket. *Aerospace Science and Technology.* **89**, 431-444 (2019).
11. Leccese, G., Cavallini, E., Pizzarelli, M. in *AIAA Propulsion and Energy 2019 Forum.* (2019).

12. Cardoso, K. P., Ferrão, L. F. A., Kawachi, E. Y., Gomes, J. S., Nagamachi, M. Y. Ballistic Performance of Paraffin-Based Solid Fuels Enhanced by Catalytic Polymer Degradation. *Journal of Propulsion and Power.* **35** (1), 115-124 (2019).
13. Paccagnella, E., Barato, F., Pavarin, D., Karabeyoğlu, A. Scaling Parameters of Swirling Oxidizer Injection in Hybrid Rocket Motors. *Journal of Propulsion and Power.* **33** (6), 1378-1394 (2017).
14. Kumar, R., Ramakrishna, P. A. Effect of protrusion on the enhancement of regression rate. *Aerospace Science and Technology.* **39**, 169-178 (2014).
15. Kumar, R., Ramakrishna, P. A. Enhancement of Hybrid Fuel Regression Rate Using a Bluff Body. *Journal of Propulsion and Power.* **30** (4), 909-916 (2014).
16. Degges, M. J. et al. in *49th AIAA/ASME/SAE/ASEE Joint Propulsion Conference.* (2013).
17. Connell, T., Young, G., Beckett, K., Gonzalez, D. R. in *AIAA Scitech 2019 Forum.* (2019).
18. Whitmore, S., Peterson, Z., Eilers, S. in *47th AIAA/ASME/SAE/ASEE Joint Propulsion Conference & Exhibit.* (2011).
19. Whitmore, S. A., Armstrong, I. W., Heiner, M. C., Martinez, C. J. in *2018 Joint Propulsion Conference.* (2018).
20. Whitmore, S. A., Peterson, Z. W., Eilers, S. D. Comparing Hydroxyl Terminated Polybutadiene and Acrylonitrile Butadiene Styrene as Hybrid Rocket Fuels. *Journal of Propulsion and Power.* **29** (3), 582-592 (2013).
21. Whitmore, S. A., Sobbi, M., Walker, S. in *50th AIAA/ASME/SAE/ASEE Joint Propulsion Conference.* (2014).
22. Whitmore, S. A., Walker, S. D. Engineering Model for Hybrid Fuel Regression Rate Amplification Using Helical Ports. *Journal of Propulsion and Power.* **33** (2), 398-407 (2017).
23. Creech, M. et al. in *53rd AIAA Aerospace Sciences Meeting.* (2015).
24. Lyne, J. E. et al. in *2018 Joint Propulsion Conference.* (2018).
25. Elliott, T. S. et al. in *52nd AIAA/SAE/ASEE Joint Propulsion Conference.* (2016).
26. Armold, D. et al. in *49th AIAA/ASME/SAE/ASEE Joint Propulsion Conference.* (2013).
27. Armold, D. M. et al. in *50th AIAA/ASME/SAE/ASEE Joint Propulsion Conference.* (2014).
28. Fuller, J., Ehrlich, D., Lu, P., Jansen, R., Hoffman, J. in *47th AIAA/ASME/SAE/ASEE Joint Propulsion Conference & Exhibit.* (2011).
29. Lee, C., Na, Y., Lee, J.W., Byun, Y.H. Effect of induced swirl flow on regression rate of hybrid rocket fuel by helical grain configuration. *Aerospace Science and Technology.* **11** (1), 68-76 (2007).
30. Tian, H., Li, Y., Li, C., Sun, X. Regression rate characteristics of hybrid rocket motor with helical grain. *Aerospace Science and Technology.* **68** 90-103 (2017).
31. Hitt, M. A. in *2018 Joint Propulsion Conference.* (2018).
32. Wang, Z., Lin, X., Li, F., Yu, X. Combustion performance of a novel hybrid rocket fuel grain with a nested helical structure. *Aerospace Science and Technology.* **97** (2020).

33. McBride, J. B., Gordon, S. *Computer Program for Calculation of Complex Chemical Equilibrium Compositions and APPlications.* (1996).

34. De Zilwa, S., Zilliac, G., Karabeyoglu, A., Reinath, M. in *39th AIAA/ASME/SAE/ASEE Joint Propulsion Conference and Exhibit.* (2003).

35. Franco, M. et al. Regression Rate Design Tailoring Through Vortex Injection in Hybrid Rocket Motors. *Journal of Spacecraft and Rockets.* **57** (2), 278-290 (2020).